

# Gas/Liquid Pulsed Discharge Plasma in a Slug Flow Reactor under Pressurized Argon for Dye Decomposition

Wanying Zhu, Wahyudiono, Hideki Kanda, and Motonobu Goto\*

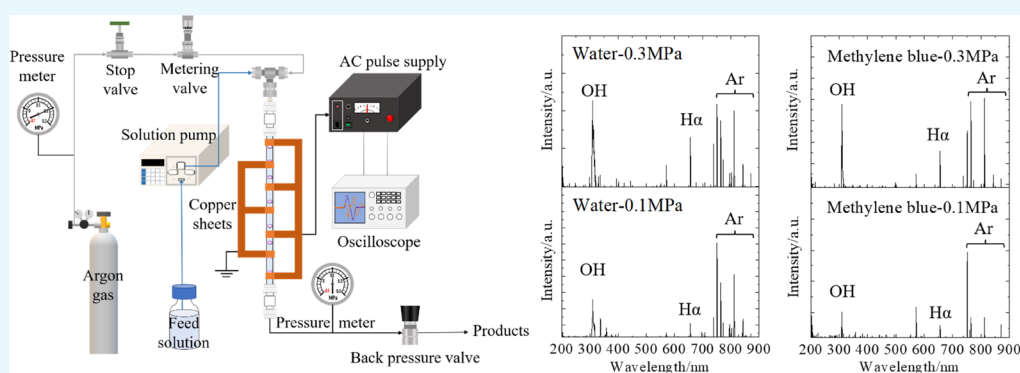
Cite This: *ACS Omega* 2022, 7, 12993–12999

Read Online

ACCESS |

Metrics &amp; More

Article Recommendations



**ABSTRACT:** Pulsed discharge plasma produced in a gas/liquid environment has attracted much attention because of its low energy requirement and the generation of various radical species with high reactivity. In our previous work, a slug flow system was developed to produce gas/liquid plasma under atmospheric pressure, generating continuous bubbles and stable gas–liquid interfaces. Currently, meaningful results have also been obtained in the field of plasma under high-pressure conditions. Therefore, in this study, a slug flow system using gas/liquid discharge plasma was implemented under pressurized argon. The system pressure was controlled from 0.1 (atmospheric pressure) to 0.4 MPa, and the effect of pressure on the system was investigated. This system was also applied to the decomposition of methylene blue. The chemical reactivity was studied, and the energy of the system was calculated. The results showed that as the system pressure increased, the decomposition rate of methylene blue decreased, while the concentration of the total oxidation species increased. This can be explained by a decrease in the energy available for methylene blue decomposition owing to the steady input energy and increasing energy loss.

## 1. INTRODUCTION

Cold plasma technology has gained immense attention because of its environmentally friendly advantages, simplicity, effectiveness, and cost-effectiveness.<sup>1,2</sup> Discharge plasma is usually easier to generate in a gas medium than in a liquid medium.<sup>3</sup> Furthermore, lower energy and operating cost are required to produce plasma in a gas/liquid environment than as a direct discharge in a liquid.<sup>4</sup> In addition, the gas–liquid interface surface area is large, making it highly effective for gaseous species to diffuse inside the liquid.<sup>5</sup> When high-voltage electrons are introduced into a gas/liquid environment, gas molecules or atoms are ionized first to form initial radicals. Then, the generated radicals make contact and react with molecules in the liquid medium via the gas/liquid interface, leading to the generation of various radical species with high reactivity in the liquid phase.<sup>6–8</sup> Based on the above advantages, gas/liquid discharge plasma has been applied in various fields, including dye treatment,<sup>9,10</sup> degradation of pharmaceutical compounds,<sup>11,12</sup> and synthesis of nanomaterials.<sup>13</sup>

Common methods to produce plasma in gas/liquid environments are to locate the electrode above the liquid surface or to immerse the electrode in the liquid.<sup>14,15</sup> The metal/metal ions vaporized from the electrode can be introduced into the liquid phase, leading to the contamination of the system. In conventional gas/liquid interface plasma reactions,<sup>16,17</sup> gas is introduced from the bottom of the tank and floated due to buoyancy, and plasma is generated inside the bubbles. These bubbles deform, coalesce to become larger, break up to become smaller, or move erratically providing a very nonuniform plasma reaction field. In addition, the treatment capacity is also limited by the tank reactor. To solve the above problem, we proposed a

Received: January 16, 2022

Accepted: March 21, 2022

Published: April 5, 2022



slug flow plasma reaction system that provides a very uniform plasma reaction field as the bubbles are not deformed and move regularly.<sup>18</sup> The slug flow plasma reaction method consisted of a continuous alternating flow of gas and feed solution through a capillary glass tube with copper electrodes on the outside. Stable plasma was produced when uniform bubbles flowed through the electrodes at a high voltage. This system provides an easy, continuous, and environmentally friendly process and has been applied successfully for the decomposition of methyl blue<sup>19</sup> and synthesis of silver nanoparticles<sup>20</sup> and cerium dioxide nanoparticles.<sup>21</sup> However, this system has only been applied under atmospheric pressure.

Research on plasma under higher pressure is relatively rare, but meaningful results have been obtained in this reaction field. Sasaki et al.<sup>22</sup> reported that the electron temperature increased with the increase in discharge pressure in microwave helium plasma. One of the reasons for this is the production of electrons with medium energy through heavy particle collisions at a high gas pressure. Hayashi et al.<sup>23</sup> reported that after applying high-voltage discharge plasma in a gas/liquid environment with a copper rod as an electrode, carbon solid materials were only generated under high-pressure conditions. Furthermore, Wahyudiono et al.<sup>24</sup> reported that the conversion rate of pyrrole increased with increasing reaction pressure. This may be due to the high voltage required for the gas breakdown under higher-pressure conditions, which led to higher energy on plasma generation, and as the pressure increased, dissolution of gas and active species in the liquid phase also increased. Therefore, it suggests that reactions in the plasma fields may be more active under higher-pressure conditions. Hence, it is worth investigating the gas/liquid plasma system under high pressure. However, new challenges have arisen due to the high voltage requirement for gas breakdown and difficulty in maintaining discharge plasma under high-pressure conditions.

In this study, we implemented a slug flow system using gas/liquid discharge plasma under pressurized argon by combining slug flow plasma technology with high-pressure plasma technology. Further insight into the chemical reactivity and energy calculations of the system was also gained. Additionally, this system was applied for the decomposition of methylene blue. Methylene blue is a pollutant commonly present in textile wastewater, causing severe environmental and health problems.<sup>25</sup> This chemical is difficult to degrade by traditional treatments because of its complex and stable structure.<sup>26</sup> As an advanced oxidation process, plasma technologies have shown specific advantages in the in situ generation of strong oxidants and the absence of byproducts.<sup>27</sup>

## 2. MATERIALS AND METHODS

**2.1. Materials.** Methylene blue ( $C_{16}H_{18}N_3SCl$ ), sodium chloride (NaCl, 99.5%), potassium iodide (KI, 99.5%), sodium thiosulfate pentahydrate ( $Na_2S_2O_3 \cdot 5H_2O$ ), starch (product no.191-03985), and distilled water (product no. 049-16787) were purchased from Wako Pure Chemical Industries, Ltd., Osaka, Japan. Argon (purity >99.99%) was purchased from Sogo Kariya Sanso, Inc., Nagoya, Japan. All chemicals used in this study were used as received without further purification.

**2.2. Experimental Methods.** Figure 1 shows a schematic of the slug flow system with pulsed discharge plasma under pressurized argon. A straight capillary glass tube (300 mm  $\times$  2.0 mm i.d., Fujirika Kogyo Co., FPT-300, Osaka, Japan) was used as the slug flow reactor. Bubbles and gas/liquid interfaces were generated by flowing gas and feed solution through a T-type

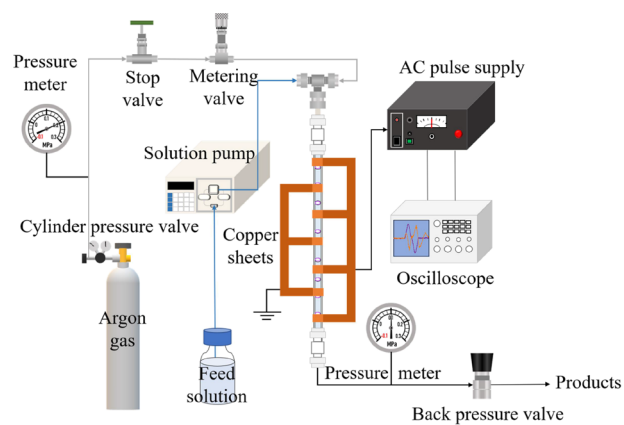


**Figure 1.** Apparatus of the slug flow system with pulsed discharge plasma under pressurized conditions.

junction (SS-200-3, Swagelok) simultaneously. The flow rates of the gas and feed solution were controlled using a metering valve and a high-performance liquid chromatography solution pump (LC-10AD, Shimadzu Co., Kyoto, Japan), respectively. Copper (Cu) sheets of 1 cm width were attached to the outer capillary glass tube as electrodes. Seven electrodes, including four high-voltage electrodes and three ground electrodes, were arranged. The distance between the adjacent electrodes was approximately 25 mm.

Similar to the system under atmospheric pressure, components for controlling and observing the system pressure were added. The system pressure was varied from 0.1 MPa (atmosphere) to 0.4 MPa by a back pressure valve and could be observed by a pressure meter. The feed solution was flowed into the system by a solution pump, while argon gas was introduced from the stop valve. The inlet pressure was controlled by a cylinder pressure valve. A high voltage of 11 kV was introduced into the system using an AC pulse supply (TE-HVP1510K300-NP, Tamaoki Electronics Co., Ltd., Kawaguchi, Japan). A 15 mg/L methylene blue solution was used as the feed solution, and sodium chloride was added to provide a conductivity of approximately 1 mS/cm. The flow rates of the feed solution and argon gas were approximately 1.5 and 1.3 mL/min. At higher pressures, the gas density increased in proportion to the pressure. The residence time of plasma-state bubbles was controlled to be similar by adjusting the flow rate of argon under different pressures, which was approximately 20 s. Products were taken after operating the process for at least 30 min to make the plasma generation stable, and each sample contained a minimum of 15 mL.

**2.3. Analysis Methods.** Cold plasma is characterized by the fact that the temperature of heavy species is close to room temperature,<sup>28</sup> which is one of its advantages. Hence, the thermal temperature of the slug flow plasma reaction field under high pressure was measured using a compact thermal imaging camera (FLIR C3-X, Teledyne FLIR LLC, Wilsonville, USA).

The feed solution and products after plasma treatment with methylene blue were characterized using an ultraviolet–visible spectrophotometer (UV–vis; V-550, Jasco Corporation, Japan). The dye decomposition rates were calculated using the characteristic peak of methylene blue at approximately 664 nm,<sup>29,30</sup> and the intensity of the peak was directly proportional to its concentration. The decomposition rates can be calculated using eq 1 by applying the ratio of peak intensities of the feed solution and products.

$$\text{Decomposition rate} = \left[ 1 - \frac{A_p}{A_f} \right] \times 100\% \quad (1)$$

where  $A_p$  and  $A_f$  are the peak intensities of the products under different pressures and feed solution at 664 nm, respectively.

The optical emission spectra were measured approximately 1 cm above the middle of the capillary glass tube. The spectra were observed as plasma-state bubbles that flowed through the detector. Water and methylene blue aqueous solution with NaCl for providing conductivity was used as feed solution under 0.1 and 0.3 MPa, respectively. To measure the energy input, the voltage and current of the system were observed using an oscilloscope (TDS2024C, Tektronix Inc., OR, USA). A high-resolution optical fiber spectrometer linked to a computer running OPwave+ and an HR4000 (Ocean Insight, Tokyo, Japan) for the optical emission spectral analysis were also used.

### 3. RESULTS AND DISCUSSION

**3.1. Thermal Temperature of the Slug Flow Plasma System.** The highest reactor temperature, approximately 41 °C under 0.4 and 0.1 MPa, was observed by a thermal imaging camera (Figure 2), which was slightly higher than room

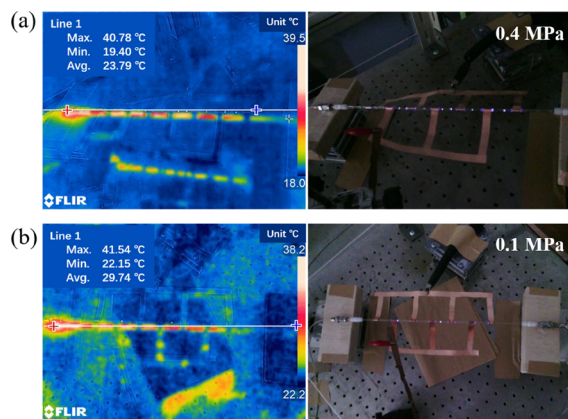


**Figure 2.** Thermal images and visible images of the system under (a) 0.4 MPa and (b) 0.1 MPa.

temperature. This indicated that even under high pressure, the system temperature was acceptably cold, and the pressure had no significant effect on the system temperature.

**3.2. Dye Decomposition Rate of Methylene Blue.** Initially, a slug flow reactor with three electrodes, including two ground electrodes and one high-voltage electrode (Figure 3a), was applied to this system. The dye decomposition rates of methylene blue under different pressures are listed in Table 1 from which it can be observed that the rates were low. According to our previous study,<sup>21</sup> the concentration of reactive species generated by plasma increases with an increase in the number of electrodes. Therefore, the number of electrodes was increased to seven, including three ground electrodes and four high-voltage electrodes (Figure 3b). The UV–vis spectra of the feed solution and products after plasma treatment using seven electrodes under different pressures are shown in Figure 4. As shown in Table 2, there was a significant increase in the methylene blue dye decomposition rate. Hence, the reactor with seven electrodes was used in all subsequent experiments.

According to the results in Tables 1 and 2, the decomposition rate of methylene blue decreased as pressure increased, which was inconsistent with our expectations. To gain further insight

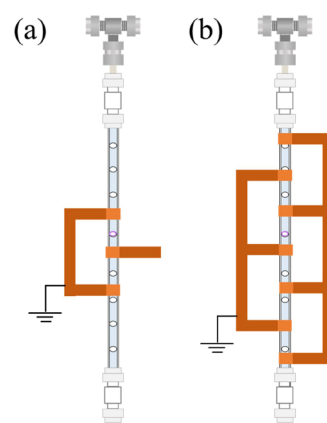


**Figure 3.** Slug flow reactors with (a) three (two ground and one high-voltage) electrodes and (b) seven (three ground and four high-voltage) electrodes.

**Table 1.** Decomposition Rate of Methylene Blue with Three Electrodes

pressure/MPa	electrode number	decomposition rate/%
0.1	3	20.25
0.2	3	13.72
0.3	3	9.95

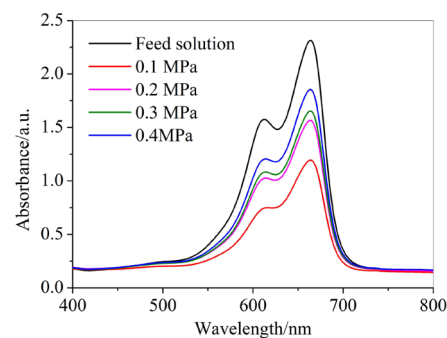


**Figure 4.** UV–vis spectra of solution and products under different pressures with seven electrodes.

**Table 2.** Decomposition Rate of Methylene Blue with Seven Electrodes

pressure/MPa	electrode number	decomposition rate/%
0.1	7	48.42
0.2	7	32.36
0.3	7	28.57
0.4	7	19.89

into the chemical reactivity of this system under pressurized argon, the reactive species generated by plasma were qualitatively and quantitatively analyzed, and the input energy was calculated. The reasons for the inconsistent result have been analyzed in a later section.

**3.3. Reactive Species.** **3.3.1. Qualitative Analysis.** In the gas/liquid plasma system, various radical species and molecules with high reactivity were generated. High-voltage electrons accelerated in a high local electric field and ionized gas molecules or atoms to form initial radicals when pulsed discharge plasma was introduced into the system.<sup>31</sup> The generated radicals then made contact with the water interface and reacted with the water molecules.<sup>32</sup> More types of radical species and molecules were

generated, including hydrogen radicals and hydroxyl radicals<sup>33,34</sup> that played an important role in subsequent reactions.

As shown in Figure 5, there was no significant change in the types of reactive species with increasing pressure. The presence

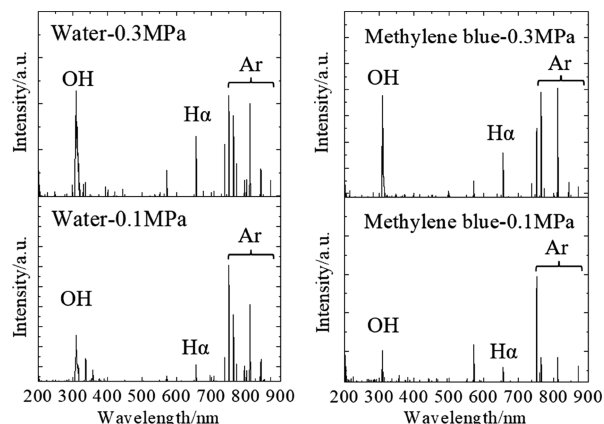


**Figure 5.** Optical emission spectrum from pulsed discharge plasma at 0.1 and 0.3 MPa.

of argon atomic system lines,<sup>35</sup> hydroxyl radicals,<sup>36</sup> and hydrogen radicals<sup>37</sup> was revealed under all conditions. However, their relative peak intensities were different. The peak intensities of OH<sup>•</sup> and H<sup>•</sup> increased compared to that of Ar<sup>•</sup> radicals, indicating the increase in the relative concentration of OH<sup>•</sup> and H<sup>•</sup> radicals with the increase in system pressure. This implies that higher pressure may be favorable for the generation and reaction of free radicals in this system. This result is verified by quantitative analysis in the next section.

**3.3.2. Quantitative Analysis.** In the gas/liquid plasma system, ionized Ar<sup>•</sup> radicals reacted with water molecules to generate OH<sup>•</sup> and H<sup>•</sup> radicals. OH<sup>•</sup> radicals continued to combine to form powerful oxidants, including oxygen, hydrogen peroxide, and ozone.<sup>38–40</sup> Therefore, the concentration of reactive species in the system could be determined in terms of the total oxidation species through iodimetry. The results for the concentration of total oxidation species under different pressures are shown in Table 3.

**Table 3. Concentration of Total Oxidation Species under Different Pressures**

pressure/MPa	<i>c</i> [oxidization species]/mM
0.1	0.12
0.2	0.21
0.3	0.25
0.4	0.29

As shown in Table 3, the concentration of total oxidation species increased as the system pressure increased, which is consistent with the results of the optical emission spectra. This indicated that the pressurized conditions were beneficial for the generation of radical species in this system. The generation processes of oxidation species are shown in reactions R1R2R3R4R5R6.<sup>19,32,33</sup> As the pressure increased and more argon was introduced into the system, the probability of collisions between electrons and argon atoms increased. More argon atoms were ionized, leading to the increase in the generated Ar<sup>•</sup> radicals, as shown in reaction R1. Meanwhile, the density of the feed solution also increased, resulting in an

increase in the number of water molecules that came in contact and reacted with the increased number of initial Ar<sup>•</sup> radical species. This improved the reactions to produce more OH<sup>•</sup> and H<sup>•</sup> radicals, as shown in reaction R2. The increase in the generated OH<sup>•</sup> radicals also led to an increase in the concentration of oxidants that were further generated, as shown in reactions R3R4R5R6. Jiang et al.<sup>41</sup> found that more reactive species were generated with increasing gas velocity because more gas molecules were broken down by energetic electrons within the same time span. Wu et al.<sup>42</sup> also reported that the ozone generation rate increased with an increase in the air flow rate in a dielectric barrier discharge plasma system, which was also due to the promoted collision between electrons and gas molecules. In addition, plasma generated in the argon phase near the gas/liquid interface then produced radical species dissolved and reacted in the liquid phase. As the system pressure and gas density increased, solubility of argon and generated active species in the liquid increased, which was also beneficial for the subsequent reactions.



Theoretically, oxidation species are dominant in the decomposition of methylene blue. Therefore, the dye decomposition rate of methylene blue is expected to increase with the increase in the concentration of the total oxidation species. However, the results showed that as the system pressure increased, the decomposition rate of methylene blue decreased. Hence, an explanation through energy calculation was attempted.

**3.4. Energy Calculation.** According to Paschen's law,<sup>43</sup> when the gas pressure continues to increase above a specific value, the required breakdown voltage increases. Initially, a high voltage of 10 kV was introduced into the system, but the plasma was difficult to generate and unstable with increasing pressure. Hence, the input voltage under different system pressures was supplied at a uniform 11 kV to maintain a single variable. The voltage discharge waveforms and current discharge waveforms are shown in Figures 6 and 7, respectively, based on which the input energy could also be calculated.

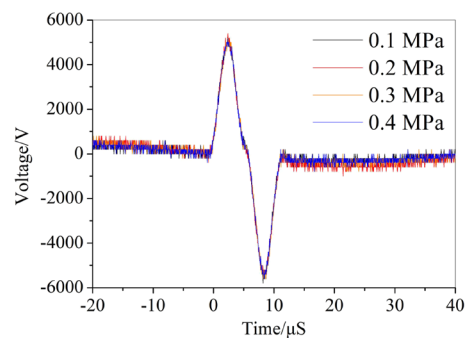


**Figure 6.** Voltage discharge waveforms under different pressures.

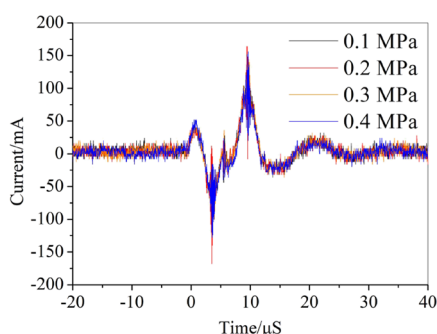


**Figure 7.** Current discharge waveforms under different pressures.

Regarding the pulsed discharge plasma supply, the pulse energy is calculated by the time integration of the voltage and current of the plasma reactor (eq R2). The discharge energy is the product of the pulse energy and pulse frequency<sup>44</sup> (eq R3). Combined with the data on dye decomposition rates calculated in previous sections, energy efficiency can be calculated<sup>45</sup> (eq R4). The calculated results are listed in Table 4.

$$\text{Pulse energy} = \int V(t) \times I(t) dt \text{ (J/pulse)} \quad (2)$$

$$\text{discharge energy} = \text{pulse energy} \times \text{pulse frequency (J/s)} \quad (3)$$

$$\text{energy efficiency} = \frac{C_0 \text{ (g/L)} \times Q \text{ (L/h)} \times \text{decomposition rate (\%)} \times \frac{1}{100}}{\text{discharge energy (kW)}} \quad (4)$$

**Table 4.** Input Energy Calculation under Different Pressures

entry	pressure/MPa	energy/W	average/W	energy efficiency/g·kWh <sup>-1</sup>
1	0.1	15.05	15.18	0.044
2		15.31		
3		15.18		
4	0.2	15.84	16.03	0.029
5		15.91		
6		16.33		
7	0.3	15.63	15.73	0.026
8		15.79		
9		15.75		
10	0.4	14.09	14.42	0.018
11		14.53		
12		14.65		

where  $C_0$  and  $Q$  are the concentration and flow rate of methylene blue, respectively.

As Table 4 shows, the input energy was maintained at a steady state and did not change significantly with increasing system pressure, and the energy efficiency of methylene blue decomposition decreased. Decomposition of methylene blue occurs mainly due to ring-breaking reactions that generate small molecular compounds.<sup>11</sup> Theoretically, as the system pressure increases, the distribution density of the gas molecules or atoms increases, resulting in an increase in collisions between the electrons and gas molecules or atoms. Excitation or ionization of molecules or atoms caused by inelastic collisions is promoted and more reactive species are generated, leading to increased collisional energy loss.<sup>46</sup> In addition, when high-voltage

discharge plasma was introduced into the gas/liquid environment, physical effects, including shock wave generation, UV radiation, and strong electrical field, were also observed.<sup>33,47,48</sup>

Under high-pressure conditions, the emission intensity of the pulsed discharge plasma was high,<sup>4</sup> which may have also increased the energy loss. Meanwhile, because water demonstrates high absorption in the vacuum UV region, direct photooxidation of a dye in water was very limited.<sup>49</sup> This result indicated that the enhanced UV also had no significant effect on the decomposition of methylene blue.

Total input energies remaining constant, the energy loss increased with increasing system pressure, resulting in a decrease in the energy available for the decomposition of methylene blue. Feng et al.<sup>50</sup> reported that the degradation efficiency of diuron increased as the input power intensity increased. Wang et al.<sup>51</sup> also reported that the removal rate of acid orange increased with the increase in energy acting to degrade organic compounds in water. Therefore, the decrease in the methylene blue decomposition rate may be due to the limited energy available under high-pressure conditions.

#### 4. CONCLUSIONS

In this study, a slug flow system using a gas/liquid pulsed discharge plasma was successfully implemented under pressurized argon, providing a novel reaction field. The chemical reactivity of this system under high-pressure conditions was also investigated for further insights. The main findings of the study are as follows:

1. The slug flow system provided a continuous reaction field in the gas/liquid discharge plasma environment under high-pressure conditions. When the system was applied to the decomposition of methylene blue, the dye decomposition rate decreased with increasing system pressure.
2. Qualitative and quantitative analyses of reactive species generated in the system were conducted. The results showed that the concentration of total oxidation species increased as the system pressure increased.
3. The input energy was calculated and maintained at a steady state under different pressure conditions. When the energy loss increased with the system pressure, the energy available for methylene blue decomposition was limited, leading to a decrease in the decomposition rate.

With the input energy remaining constant, methylene blue decomposition via the slug flow system became less effective under high-pressure conditions. However, a high concentration of total oxidation species was detected, demonstrating the system's potential for application in other reactions. There is also a possibility of higher efficiency when increasing the input energy, which needs to be studied further.

#### AUTHOR INFORMATION

##### Corresponding Author

Motonobu Goto – Department of Materials Process Engineering, Nagoya University, Nagoya 464-8603, Japan; [orcid.org/0000-0003-3219-5028](https://orcid.org/0000-0003-3219-5028); Email: [goto.motonobu@material.nagoya-u.ac.jp](mailto:goto.motonobu@material.nagoya-u.ac.jp)

##### Authors

Wanying Zhu – Department of Materials Process Engineering, Nagoya University, Nagoya 464-8603, Japan; [orcid.org/0000-0001-6174-5901](https://orcid.org/0000-0001-6174-5901)

Wahyudiono – Department of Materials Process Engineering, Nagoya University, Nagoya 464-8603, Japan; [orcid.org/0000-0003-0339-1740](https://orcid.org/0000-0003-0339-1740)

Hideki Kanda – Department of Materials Process Engineering, Nagoya University, Nagoya 464-8603, Japan; [orcid.org/0000-0002-8393-4276](https://orcid.org/0000-0002-8393-4276)

Complete contact information is available at:  
<https://pubs.acs.org/10.1021/acsomega.2c00320>

## Notes

The authors declare no competing financial interest.

## ACKNOWLEDGMENTS

This work was supported by JSPS KAKENHI (Grant Number JP20H02515) and JST SICORP (Grant Number JPMJSC18H1), Japan.

## REFERENCES

- (1) Charoux, C. M.; Patange, A.; Lamba, S.; O'Donnell, C. P.; Tiwari, B. K.; Scannell, A. G. Applications of nonthermal plasma technology on safety and quality of dried food ingredients. *J. Appl. Microbiol.* **2021**, *130*, 325–340.
- (2) Shi, J.; Bian, W.; Yin, X. Organic contaminants removal by the technique of pulsed high-voltage discharge in water. *J. Hazard. Mater.* **2009**, *171*, 924–931.
- (3) Nijdam, S.; van Veldhuizen, E.; Bruggeman, P.; Ebert, U., An Introduction to Nonequilibrium Plasmas at Atmospheric Pressure. *Plasma Chemistry and Catalysis in Gases and Liquids*; Wiley-VCH Verlag GmbH & Co. KGaA, 2012; 1–44.
- (4) Diono, W.; Machmudah, S.; Kanda, H.; Zhao, Y.; Goto, M. Pulsed Discharge Plasma in High-Pressure Environment for Water Pollutant Degradation and Nanoparticle Synthesis. *Plasma* **2021**, *4*, 309–331.
- (5) Zeghioud, H.; Nguyen-Tri, P.; Khezami, L.; Amrane, A.; Assadi, A. A. Review on discharge Plasma for water treatment: mechanism, reactor geometries, active species and combined processes. *J. Water Process Eng.* **2020**, *38*, No. 101664.
- (6) Cao, Y.; Qu, G.; Li, T.; Jiang, N.; Wang, T. Review on reactive species in water treatment using electrical discharge plasma: formation, measurement, mechanisms and mass transfer. *Plasma Sci. Technol.* **2018**, *20*, 103001.
- (7) Kanazawa, S.; Kawano, H.; Watanabe, S.; Furuki, T.; Akamine, S.; Ichiki, R.; Ohkubo, T.; Kocik, M.; Mizeraczyk, J. Observation of OH radicals produced by pulsed discharges on the surface of a liquid. *Plasma Sources Sci. Technol.* **2011**, *20*, No. 034010.
- (8) Marotta, E.; Schiorlin, M.; Ren, X.; Rea, M.; Paradisi, C. Advanced oxidation process for degradation of aqueous phenol in a dielectric barrier discharge reactor. *Plasma Processes Polym.* **2011**, *8*, 867–875.
- (9) Xin, Y.-Y.; Zhou, L.; Ma, K.-K.; Lee, J.; Qazi, H.; Li, H.-P.; Bao, C.-Y.; Zhou, Y.-X. Removal of bromoamine acid in dye wastewater by gas-liquid plasma: The role of ozone and hydroxyl radical. *J. Water Process Eng.* **2020**, *37*, No. 101457.
- (10) Nau-Hix, C.; Holsen, T. M.; Thagard, S. M. Influence of solution electrical conductivity and ionic composition on the performance of a gas-liquid pulsed spark discharge reactor for water treatment. *J. Appl. Phys.* **2021**, *130*, No. 123301.
- (11) Corella Puertas, E.; Peyot, M.-L.; Pineda, M.; Volk, K.; Coulombe, S.; Yargeau, V. Degradation of diatrizoate in a pin-to-liquid plasma reactor, its transformation products and their residual toxicity. *Sci. Total Environ.* **2021**, *782*, No. 146895.
- (12) Wang, X.; Luo, J.; Huang, Y.; Mei, J.; Chen, Y. Degradation of pharmaceutical contaminants by bubbling gas phase surface discharge plasma combined with gC 3 N 4 photocatalysis. *Environ. Sci.: Water Res. Technol.* **2021**, *7*, 610–621.
- (13) Nguyen, L. N.; Lamichhane, P.; Choi, E. H.; Lee, G. J. Structural and Optical Sensing Properties of Nonthermal Atmospheric Plasma-Synthesized Polyethylene Glycol-Functionalized Gold Nanoparticles. *Nanomaterials* **2021**, *11*, 1678.
- (14) Lin, L.; Ma, X.; Li, S.; Wouters, M.; Hessel, V. Plasma-electrochemical synthesis of europium doped cerium oxide nanoparticles. *Front. Chem. Sci. Eng.* **2019**, *13*, 501–510.
- (15) Shen, J.; Zhang, H.; Xu, Z.; Zhang, Z.; Cheng, C.; Ni, G.; Lan, Y.; Meng, Y.; Xia, W.; Chu, P. K. Preferential production of reactive species and bactericidal efficacy of gas-liquid plasma discharge. *Chem. Eng. J.* **2019**, *362*, 402–412.
- (16) Sato, K.; Yasuoka, K. Pulsed Discharge Development in Oxygen, Argon, and Helium Bubbles in Water. *IEEE Trans. Plasma Sci.* **2008**, *36*, 1144–1145.
- (17) Tachibana, K.; Takekata, Y.; Mizumoto, Y.; Motomura, H.; Jinno, M. Analysis of a pulsed discharge within single bubbles in water under synchronized conditions. *Plasma Sources Sci. Technol.* **2011**, *20*, No. 034005.
- (18) Yamada, M.; Wahyudiono; Machmudah, S.; Kanda, H.; Goto, M. Nonthermal Atmospheric Pressure Plasma for Methylene Blue Dye Decolorization by Using Slug Flow Reactor System. *Plasma Chem. Plasma Process.* **2020**, *40*, 985–1000.
- (19) Wahyudiono; Mano, K.; Hayashi, Y.; Yamada, M.; Takahashi, S.; Takada, N.; Kanda, H.; Goto, M. Atmospheric-pressure pulsed discharge plasma in capillary slug flow system for dye decomposition. *Chem. Eng. Process.* **2019**, *135*, 133–140.
- (20) Yamada, M.; Takahashi, S.; Wahyudiono; Takada, N.; Kanda, H.; Goto, M. Synthesis of silver nanoparticles by atmospheric-pressure pulsed discharge plasma in a slug flow system. *Jpn. J. Appl. Phys.* **2019**, *58*, No. 016001.
- (21) Zhu, W.; Lin, Y.; Zhu, L.; Wahyudiono; Honda, M.; Kanda, H.; Goto, M. Synthesis of Cerium Dioxide Nanoparticles by Gas/Liquid Pulsed Discharge Plasma in a Slug Flow Reactor. *ACS Omega* **2021**, *6*, 20966–20974.
- (22) Sasaki, K.; Soma, S.; Akashi, H.; ElSabbagh, M.; Ikeda, Y. *Electron Temperatures and Electron Densities in Microwave Helium Discharges with Pressures Higher than 0.1 MPa*; Wiley Online Library 2015.
- (23) Hayashi, Y.; Takada, N.; Wahyudiono; Kanda, H.; Goto, M. One-step synthesis of water-dispersible carbon nanocapsules by pulsed arc discharge over aqueous solution under pressurized argon. *Res. Chem. Intermed.* **2017**, *43*, 4201–4211.
- (24) Wahyudiono; Watanabe, H.; Machmudah, S.; Kiyan, T.; Sasaki, M.; Akiyama, H.; Goto, M. Pyrrole conversion induced pulse discharge plasma over a water surface under high-pressure argon. *Chem. Eng. Process.* **2012**, *61*, 51–57.
- (25) He, P. Y.; Zhang, Y. J.; Chen, H.; Liu, L. C. Development of an eco-efficient CaMoO<sub>4</sub>/electroconductive geopolymer composite for recycling silicomanganese slag and degradation of dye wastewater. *J. Clean. Prod.* **2019**, *208*, 1476–1487.
- (26) Tichonovas, M.; Krugly, E.; Racys, V.; Hippler, R.; Kauneliene, V.; Stasiulaitiene, I.; Martuzevicius, D. Degradation of various textile dyes as wastewater pollutants under dielectric barrier discharge plasma treatment. *Chem. Eng. J.* **2013**, *229*, 9–19.
- (27) Oturan, M. An ecologically effective water treatment technique using electrochemically generated hydroxyl radicals for in situ destruction of organic pollutants: application to herbicide 2, 4-D. *J. Appl. Electrochem.* **2000**, *30*, 475–482.
- (28) Tabares, F. L.; Junkar, I. Cold Plasma Systems and their Application in Surface Treatments for Medicine. *Molecules* **2021**, *26*, 1903.
- (29) Chang, H.; Su, C.; Lo, C.-H.; Chen, L.-C.; Tsung, T.-T.; Jwo, C.-S. Photodecomposition and surface adsorption of methylene blue on TiO<sub>2</sub> nanofluid prepared by ASNSS. *Mater. Trans.* **2004**, *45*, 3334–3337.
- (30) Jiao, Q.; Liu, Q. Characterization of the interaction between methylene blue and glycosaminoglycans. *Spectrochim. Acta, Part A* **1999**, *55*, 1667–1673.
- (31) Joshi, R. P.; Thagard, S. M. Streamer-Like Electrical Discharges in Water: Part II. Environmental Applications. *Plasma Chem. Plasma Process.* **2013**, *33*, 17–49.
- (32) Ognier, S.; Iya-Sou, D.; Fourmond, C.; Cavadias, S. Analysis of mechanisms at the plasma-liquid interface in a gas-liquid discharge

reactor used for treatment of polluted water. *Plasma Chem. Plasma Process.* **2009**, *29*, 261–273.

(33) Locke, B. R.; Sato, M.; Sunka, P.; Hoffmann, M. R.; Chang, J. S. Electrohydraulic Discharge and Nonthermal Plasma for Water Treatment. *Ind. Eng. Chem. Res.* **2006**, *45*, 882–905.

(34) Locke, B. R.; Lukes, P.; Brisset, J.-L., Elementary Chemical and Physical Phenomena in Electrical Discharge Plasma in Gas–Liquid Environments and in Liquids. *Plasma Chemistry and Catalysis in Gases and Liquids*; Wiley-VCH Verlag GmbH & Co. KGaA, 2012; 185–241.

(35) García, M. C.; Mora, M.; Esquivel, D.; Foster, J. E.; Rodero, A.; Jiménez-Sanchidrián, C.; Romero-Salguero, F. J. Microwave atmospheric pressure plasma jets for wastewater treatment: degradation of methylene blue as a model dye. *Chemosphere* **2017**, *180*, 239–246.

(36) Huang, F.; Chen, L.; Wang, H.; Yan, Z. Analysis of the degradation mechanism of methylene blue by atmospheric pressure dielectric barrier discharge plasma. *Chem. Eng. J.* **2010**, *162*, 250–256.

(37) Potocký, Š.; Saito, N.; Takai, O. Needle electrode erosion in water plasma discharge. *Thin Solid Films* **2009**, *518*, 918–923.

(38) Chu, P. K.; Lu, X., *Low temperature plasma technology: methods and applications*; CRC Press: 2013.

(39) Sun, B.; Aye, N. N.; Gao, Z.; Lv, D.; Zhu, X.; Sato, M. Characteristics of gas-liquid pulsed discharge plasma reactor and dye decoloration efficiency. *J. Environ. Sci.* **2012**, *24*, 840–845.

(40) Lu, N.; Li, J.; Wu, Y.; Masayuki, S. Treatment of Dye Wastewater by Using a Hybrid Gas/Liquid Pulsed Discharge Plasma Reactor. *Plasma Sci. Technol.* **2012**, *14*, 162–166.

(41) Jiang, B.; Zheng, J.; Liu, Q.; Wu, M. Degradation of azo dye using non-thermal plasma advanced oxidation process in a circulatory airtight reactor system. *Chem. Eng. J.* **2012**, *204-206*, 32–39.

(42) Wu, L.; Xie, Q.; Lv, Y.; Wu, Z.; Liang, X.; Lu, M.; Nie, Y. Degradation of Methylene Blue via Dielectric Barrier Discharge Plasma Treatment. *Water* **2019**, *11*, 1818.

(43) Babich, L.; Loiko, T. V. Generalized Paschen's Law for Overvoltage Conditions. *IEEE Trans. Plasma Sci.* **2016**, *44*, 3243–3248.

(44) Okumoto, M.; Mizuno, A. Conversion of methane for higher hydrocarbon fuel synthesis using pulsed discharge plasma method. *Catal. Today* **2001**, *71*, 211–217.

(45) Malik, M. A. Water Purification by Plasmas: Which Reactors are Most Energy Efficient? *Plasma Chem. Plasma Process.* **2010**, *30*, 21–31.

(46) Atomic Collisions. *Principles of Plasma Discharges and Materials Processing*; John Wiley & Sons, 2005; 43–85.

(47) Abramov, V. O.; Abramova, A. V.; Cravotto, G.; Nikonov, R. V.; Fedulov, I. S.; Ivanov, V. K. Flow-mode water treatment under simultaneous hydrodynamic cavitation and plasma. *Ultrason. Sonochem.* **2021**, *70*, No. 105323.

(48) Sun, B.; Xin, Y.; Zhu, X.; Gao, Z.; Yan, Z.; Ohshima, T. Effects of shock waves, ultraviolet light, and electric fields from pulsed discharges in water on inactivation of *Escherichia coli*. *Bioelectrochemistry* **2018**, *120*, 112–119.

(49) Sugiarto, A. T.; Ito, S.; Ohshima, T.; Sato, M.; Skalny, J. D. Oxidative decoloration of dyes by pulsed discharge plasma in water. *J. Electroanal. Chem.* **2003**, *58*, 135–145.

(50) Feng, J.; Zheng, Z.; Luan, J.; Li, K.; Wang, L.; Feng, J. Gas–liquid hybrid discharge-induced degradation of diuron in aqueous solution. *J. Hazard. Mater.* **2009**, *164*, 838–846.

(51) Wang, H.; Li, J.; Quan, X. Decoloration of azo dye by a multi-needle-to-plate high-voltage pulsed corona discharge system in water. *J. Electroanal. Chem.* **2006**, *64*, 416–421.